Article **Journal of Research and Development**
June 2022, Vol.8 No.21 6-13

Design process for dual coplanar waveguide directional couplers for power transmission

Proceso de diseño de acopladores direccionales con guía de onda coplanar diferencial para transmisión de potencia

CASTAÑEDA-IBARRA, Víctor R.†, CISNEROS-SINENCIO, Luis F.*, GARCÍA-VITE, Pedro M. and CASTILLO-GUTIÉRREZ, Rafael

Tecnológico Nacional de México, Instituto Tecnológico de Ciudad Madero, Mexico.

ID 1st Author: *Víctor Rodrígo, Castañeda-Ibarra* / **ORC ID:** 0000-0003-3863-0553, **CVU CONACYT ID:** 1083997

ID 1st Co-author: *Luis Fortino, Cisneros-Sinencio* / **CVU CONACYT ID:** 102695

ID 2nd Co-author: *Pedro Martín, García-Vite* / **ORC ID:** 0000-0001-6019-7958, **CVU CONACYT ID:** 227310

ID 3rd Co-author: *Rafael, Castillo-Gutiérrez* / **ORC ID:** 0000-0001-8599-892X, **CVU CONACYT ID:** 63299

DOI: 10.35429/JRD.2022.21.8.6.13 Received: January 20, 2022; Accepted: May 30, 2022

Abstract

In this paper, a design process for power directional couplers using dual conductor-backed coplanar waveguides (CBCPW), is presented. The proposed methodology is applied to the design of a 50 Ω impedance coupler with 10 dB coupling factor for a central frequency of 2.5 GHz. The resulting coupler is validated through simulation by obtaining its dispersion parameters using ANSYS High Frequency Structure Simulator (HFSS). From the analysis of the return loss, insertion loss and coupling factor, in a range of 1 to 4 GHz, it was found that the coupling factor complies with the design specification for frequencies from 2 to 3 GHz, with insertion losses between -1 and -2 dB around the center frequency and return losses of -15 dB.

Methodology, directional coupling, coplanar waveguide, dispersion parameters

Resumen

En este trabajo se propone un proceso de diseño para acopladores direccionales de potencia construidos con guías de onda coplanares con conductor de respaldo (CBCPW) duales. Esta propuesta se aplicará en el diseño de un acoplador con impedancia de 50 Ω y un factor de acoplamiento de 10 dB para una frecuencia central de 2.5 GHz. El proceso de diseño será validado a través de sus parámetros de dispersión obtenidos mediante el Simulador de Estructuras en Alta Frecuencia de Ansys (HFSS). De acuerdo al análisis de las gráficas de pérdidas de retorno, de pérdidas de inserción y de factor de acoplamiento, en un rango de 1 a 4 GHz, se comprobó que el factor de acoplamiento cumple con la especificación de diseño para frecuencias de 2 a 3 GHz, con pérdidas de inserción entre los -1 y -2 dB alrededor de la frecuencia central y pérdidas de retorno de -15 dB.

Metodología, acoplador direccional, guía de onda coplanar, parámetros de dispersión

Citation: CASTAÑEDA-IBARRA, Víctor R., CISNEROS-SINENCIO, Luis F., GARCÍA-VITE, Pedro M. and CASTILLO-GUTIÉRREZ, Rafael. Design of dual coplanar waveguide directional couplers for power transmisión. Journal of Research and Development. 2022. 8-21:6-13.

* Author's Correspondence (E-mail: fortino.cs@cdmadero.tecnm.mx)
† Researcher contributing as first author.

Introduction

Directional couplers are four- or three-port linear passive devices used to couple power from a transmission line to a coupled port (Avionics Department, 2013). These circuits are constructed using two transmission lines that are placed close enough to each other so that some of the power travelling on one line can be transmitted to the other line with a known attenuation; this phenomenon is known as coupling (Simons 2001). The coupled output of this device is used to obtain information from a signal without interrupting the power flow in the system, with small insertion loss due to coupling. Figure 1 shows the structure of a directional coupler along with the power flow through its ports; because they are linear devices, the distribution of its ports is arbitrary, so any port can serve as an input.

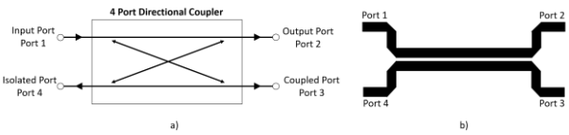

Figure 1 Directional Coupler a) Schematic and b) Structure of a directional microstrip coupler

The structure of such circuits can consist of different types of transmission lines such as: strip lines, microstrip lines and waveguides, each with different coupling capabilities (Roshani, et al., 2022). The field of application of each of these options will depend on their range of coupling values. Very weak coupling values relate to microwave power monitoring applications; for example, for sampling incident and reflected waves in reflectometers, a fundamental part of vector or scalar network analysers (Mousavi, et al., 2015). Other applications of directional couplers relate to signal distribution in antenna networks, balanced circuits and mixing applications (Liang, et al., 2007) (Shi, et al., 2008) (Shi, et al., 2010) (Chen & Xue, 2013) (Liu, et al., 2014) (Yu & Yang, 2022) (Zhao, et al., 2022).

The length of the coupled lines of a directional coupler must measure at least one quarter of the wavelength. When this condition is met, the coupling factor (k) reaches its maximum value, optimising the power transfer from the input port to the coupled port. This factor can be defined as the inverse of the fraction of voltage transferred.

Depending on the application, this factor can take different values, typically between 3 and 40 dB. Other important parameters in coupler design are the transmission factor, directivity factor and isolation factor.

- The transmission factor represents the power that is transferred from port 1 to port 2 through the main line of the structure, its ideal value expressed in dB is equal to $20\log\left|\sqrt{1-1/C^2}\right|$ dB, with a typical value of 0.5 dB.

- The directivity factor describes the magnitude of the unwanted coupling between port 1 and port 4 compared to the coupling at port 3; the higher this value, the higher the directivity of the coupler. Its typical value is 40 dB.

- The isolation factor describes how much of the power applied to port 1 is directed to port 4. Ideally this value is very high, tending towards infinity, however, in real systems, its magnitude is around 40 dB.

Characteristics of the coupled lines

Any pair of coupled transmission lines can be described as a four-port configuration, where one of the lines (or both depending on the transmission mode) carries a signal that is induced into the adjacent line, generating charges and currents on the adjacent line. Since the field pattern (mode) on the pair of lines is the result of the linear superposition of each of the individual field patterns; when they travel in the same direction it is called an even mode; and when both waves travel in the opposite direction it is called an odd mode (Edwards, 2016). Figure 2 shows the directions of both the electric field and the magnetic field for each of the modes in a coplanar line structure. It can be deduced that the behaviour of a coupled structure is the result of the superposition of the effects of both modes. Due to the difference in the distribution of fields in each mode, two different characteristic impedances are defined; one corresponding to the even mode (Z_{0e}) and the other for the odd mode (Z_{0o}).

ISSN-On line: 2444-4987

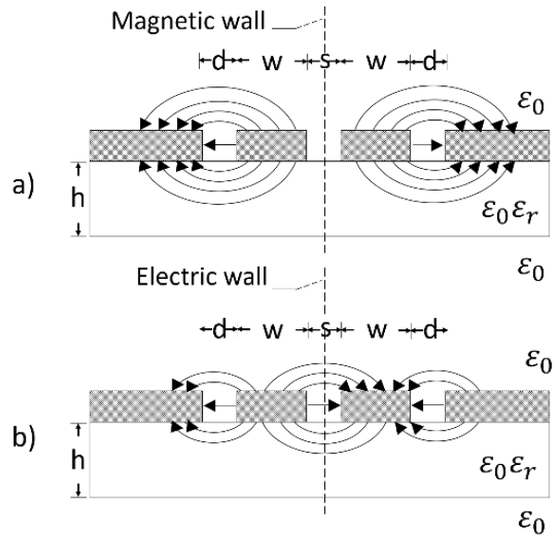

Figure 2 Direction of magnetic and electric fields in coupled lines a) Even mode and b) Odd mode

The design process of a directional coupler consists of determining the physical dimensions of a coupled line structure. The calculation of these parameters is derived from the odd and even mode impedances Z_{0e} and Z_{0o} impedances (Edwards, 2016). The ratio of these impedances to *k* and Z_{S0} se describe en (Wadell, 1991). is described in (Wadell, 1991). By solving these equations, it is possible to plot the relationship between the line impedances and their coupling factor for Z_{0s} = 50 Ω. This relationship is shown in the graph in Figure 3, where it can be seen that the closer the two impedance values, odd and even, at Z_{0s}, the coupling between lines decreases, minimising the power transfer from one line to the other. Conversely, if the difference between these values increases, so does the coupling between lines.

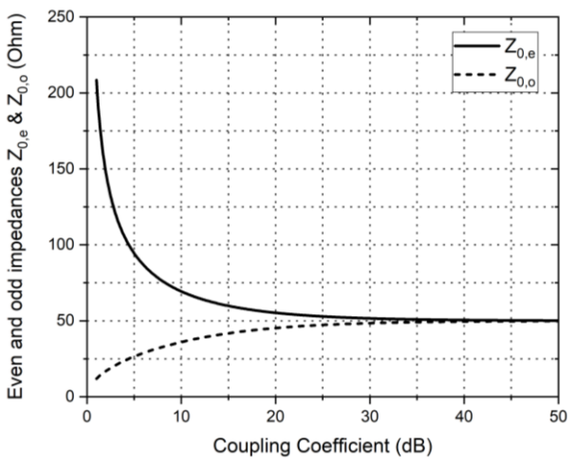

Figure 3 Even and odd mode impedance Z_{0e} and Z_{0o} (Ω) with respect to coupling coefficient *k* (dB)

The level of coupling between the two lines also depends on the length of the coupled structure, finding its maximum when the length of the line is equal to one quarter of the wavelength ($\lambda_g/4$), i.e., when the electrical length θ is equal to π/2.

Structures of a CBCPW

A coplanar waveguide (CPW) consists of a conductor line mounted on a dielectric that has a return conductor on each side of the line, both located in the same plane as the centre conductor (He, et al., 2022). A coplanar wave with backup conductor (CBCPW) is a coplanar waveguide to which an additional ground conductor is added in a second plane located on the other side of the substrate. Both waveguides share characteristics such as ease of being connected in series and shunt, low radiation and low dispersion, so they are widely used in power splitters, mixers, band-pass filters, Lange couplers, high directivity couplers and switched transmission lines (Watson & Gupta, 1997) (Kim, et al., 2002) (Tessmann, 2006) (Chen, et al., 2010) (Wane, et al., 2015) (Xiao, et al., 2016) (Du, et al., 2022).

The characteristics of a CBCPW are defined by its dimensions, being: the width of its central conductor (*2a*), the spacing between the two adjacent ground planes (*2b*), as well as the height of the substrate (*h*). Figure 4 shows the CBCPW structure with its different dimensions.

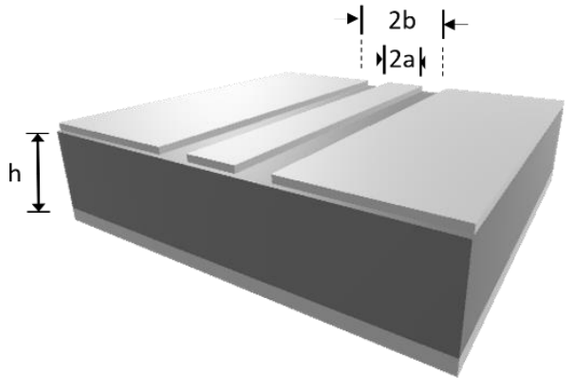

Figure 4 Cross-sectional dimensions of a coplanar waveguide with back-up conductor (*a*, *b*, *h*).

In the case of a dual CBCPW, as shown in Figure 5, there are two centre conductors. In this case, the line dimensions are: the distance between the two signal lines (*s*), the spacing to adjacent ground planes (*d*), the width of the centre conductors (*w*) and the height of the substrate (*h*).

ISSN-On line: 2444-4987

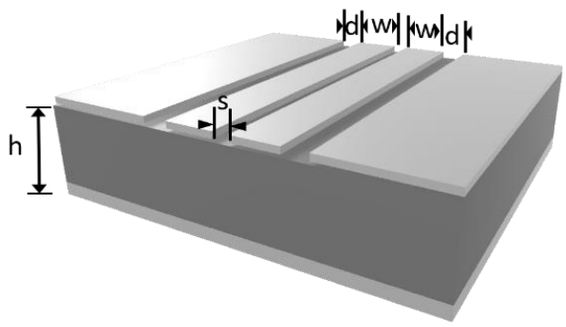

Figure 5 Cross-sectional dimensions of a dual coplanar waveguide with back-up conductor (*d*, *w*, *s*, *h*)

Characteristic impedance of a CBCPW

In (Wadell, 1991) and (Simons, 2001) the equations relating each of the dimensions of a coplanar waveguide to its impedances are described for both a CBCPW and a dual CBCPW structure. With the help of Octave mathematical software, these equations were solved to relate different line parameters. The graph in Figure 6 shows the relationship between the coupling coefficient *k* and the factor *s/(s+2w)* for different values of *[(s/2)+w]/h* with Z_{0s}=50 Ω, *h*=1.6, ε_r=4.0 and *d*=s.

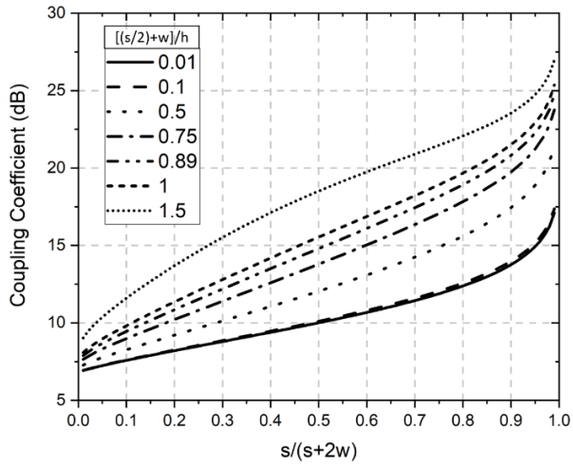

Figure 6 Coupling coefficient *k* (dB) with respect to different values of *s/(s+2w)* for different values of *[(s/2)+w]/h* with Z_{s0}=50Ω, *h*=1.6, ε_r=4.0 and with *d*=s.

The graph in Figure 7 shows the relationship between $Z_{0,e}$ and $Z_{0,o}$ for different values of *s/h* and *w/h* with *d*=*s*.

Both graphs will be useful in determining the dimensions of the coupler as a function of its k-factor and its characteristic impedance.

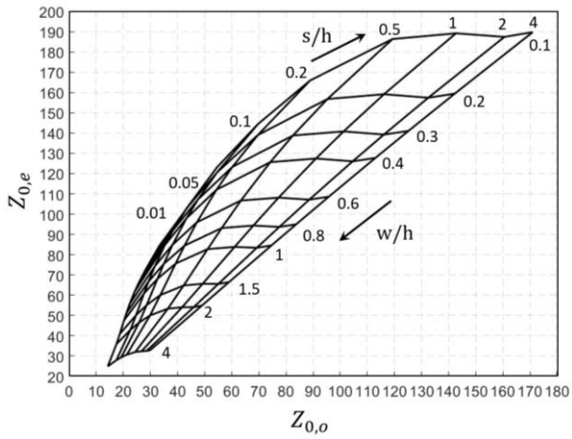

Figure 7 Odd and even mode impedances $Z_{0,e}$ and $Z_{0,e}$ with respect to different ratios of *s/h* and *w/h* with *d*=*s*.

Directional coupler design

Figure 8 shows the structure of the directional coupler of interest, where two different sections can be identified. The first section is characterised by two parallel conductor lines (constant s); for this section the design equations for a dual CBCPW will be used. In the second section, s varies continuously, so the previous equations are no longer valid; for this section, the design equations for a simple CBCPW are used. Thus, considering the coupler as three different waveguides connected in series, it is possible to ensure an impedance of 50 Ω throughout the device.

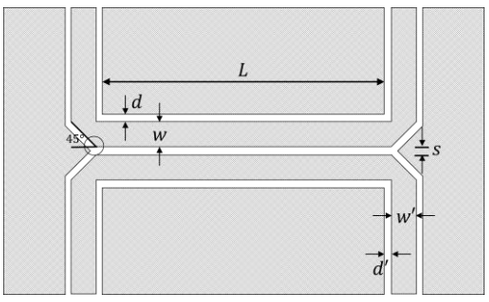

Figure 8 Physical dimensions involved in the electrical characteristics of a directional coupler using a CBCPW structure

The calculations for the construction of a Dual CBCPW with a characteristic impedance of 50 Ω and a coupling factor of 10 dB are presented below. From the graph in Figure 3 we get $Z_{0,e} = 69.269\ \Omega$ and $Z_{0,o} = 36.185\ \Omega$. In turn, with the help of graphs in Figures 6 and 7, it is found that these impedances can be achieved with a ratio s/h= 0.18 and w/h=1.18. Taking h=1.6 and $\varepsilon_r = 4.0$, corresponding to the substrate of a commercial PCB manufactured with FR-4, we have.

ISSN-On line: 2444-4987

h=1.6 s=0.3 d=0.3 w=1.91 ε_r=4.0

Once the transverse parameters have been obtained, it is necessary to calculate the length of the coupled section. For this, it is necessary to calculate the effective even and odd mode permittivities $\varepsilon_{eff,e}$ y $\varepsilon_{eff,o}$, so that:

$$r = \frac{s}{s+2w} = 0.0728 \quad (1)$$

$$k_1 = \frac{s+2w}{s+2w+2d} = 0.8729 \quad (2)$$

$$\beta_1 = \left[\frac{(1-r^2)}{(1-{k_1}^2 r^2)}\right]^{1/2} = 0.9994 \quad (3)$$

$$\Lambda = \frac{\sinh\left[\frac{\pi(\frac{s}{2}+w+d)}{2h}\right]^2}{2} = 12.6150 \quad (4)$$

$$\Lambda' = \frac{\cosh\left[\frac{\pi(\frac{s}{2}+w+d)}{2h}\right]^2}{2.0} = 13.1150 \quad (5)$$

$$t_c = \sinh\left[\frac{\pi(\frac{s}{2}+w)}{2\,h}\right]^2 - \Lambda = 1.1644 \quad (6)$$

$$t'_c = \sinh\left[\frac{\pi(\frac{s}{2}+w)}{2h}\right]^2 - \Lambda' + 1.0 = 1.6644 \quad (7)$$

$$t_B = \sinh\left(\frac{\pi\, s}{4h}\right)^2 - \Lambda = -12.5932 \quad (8)$$

$$t'_B = \sinh\left[\frac{\pi\, s}{4h}\right]^2 - \Lambda' + 1.0 = -11.9660 \quad (9)$$

$$k_o = \Lambda \frac{-\sqrt{\Lambda^2-{t_c}^2}+\sqrt{\Lambda^2-{t_B}^2}}{t_B\sqrt{\Lambda^2-{t_c}^2}+t_c\sqrt{\Lambda^2-{t_B}^2}} = 0.9477 \quad (10)$$

$$k_e = \Lambda' \frac{-\sqrt{\Lambda'^2-{t'_c}^2}+\sqrt{\Lambda'^2-{t'_B}^2}}{t'_B\sqrt{\Lambda'^2-{t'_c}^2}+t'_c\sqrt{\Lambda'^2-{t'_B}^2}} = 0.6829 \quad (11)$$

$$\varepsilon_{eff,o} = \frac{2\varepsilon_r\frac{K(k_o)}{K'(k_o)}+\frac{K(\beta_1)}{K'(\beta_1)}}{2\frac{K(k_o)}{K'(k_o)}+\frac{K(\beta_1)}{K'(\beta_1)}} = 2.5342 \quad (12)$$

$$\varepsilon_{eff,e} = \frac{2\varepsilon_r\frac{K(k_e)}{K'(k_e)}+\frac{K(\beta_1 k_1)}{K'(\beta_1 k_1)}}{2.0\frac{K(k_e)}{K'(k_e)}+\frac{K(\beta_1 k_1)}{K'(\beta_1 k_1)}} = 2.7739 \quad (13)$$

Because the two permittivities are different, to find the wavelength it is necessary to calculate the average of the two permittivities.

$$\varepsilon_{eff,avg} = \frac{\varepsilon_{eff,e}+\varepsilon_{eff,o}}{2} = \frac{2.7739+2.5342}{2} = 2.6540 \quad (14)$$

Thus, the average wavelength is:

$$\lambda_g = \frac{c}{f\sqrt{\varepsilon_{eff,avg}}} = \frac{3\cdot 10^{11}}{2.5^9\sqrt{2.654}} = 73.65\ mm \quad (15)$$

Therefore, the length of the coupler should be:

$$L = \lambda_g/4 = 18.414\ mm \quad (16)$$

Finally, the dimensions of the lines going to each of the ports are calculated using the equations for a simple CBCPW manufactured in the same commercial process with FR-4, thus $Z_{0s} = 50\ \Omega$, a=1.91, $h = 1.6$ y $\varepsilon_r = 4.0$. The following calculations are then performed:

$$k = \frac{a}{b} = (1.91)/(2.64) = 0.7235 \quad (17)$$

$$k_1 = \frac{\tanh\left(\frac{\pi a}{4h}\right)}{\tanh\left(\frac{\pi b}{4h}\right)} = 0.8529 \quad (18)$$

$$k' = \sqrt{1.0-k^2} = 0.6903 \quad (19)$$

$$k'_1 = \sqrt{1.0-{k_1}^2} = 0.5220 \quad (20)$$

ISSN-On line: 2444-4987

$$\varepsilon_{eff} = \frac{1.0 + \varepsilon_r \frac{K(k')}{K(k)} \frac{K(k_1)}{K(k'_1)}}{1.0 + \frac{K(k')}{K(k)} \frac{K(k_1)}{K(k'_1)}} = 2.66 \quad (21)$$

$$Z_0 = \frac{60\pi}{\sqrt{\varepsilon_{eff}}} \left[\frac{1.0}{\frac{K(k)}{K(k')} + \frac{K(k_1)}{K(k'_1)}} \right] = 50.087\ \Omega \quad (22)$$

The dimensions of the coupled section are shown in Table 1, while for the single waveguide section they are shown in Table 2.

Parameter	
k	3.188 (10 dB)
Z_{S0}	50 Ω
ε_r	4.0
t	0.035 mm
d	0.3 mm
w	1.91 mm
s	0.3 mm
h	1.6 mm
L	18.414 mm

Table 1 Physical and electrical parameters of the CBCPW Dual (coupled section)

Parameter	
Z_{S0}	50 Ω
ε_r	4.0
t	0.035 mm
a	1.91 mm
b	2.64 m
h	0 mm

Table 2 Physical and electrical parameters of the single CBCPW

Results

To validate the design of the directional coupler, its dispersion parameters obtained by simulation using Ansys High Frequency Structure Simulator (HFSS) will be analysed.

The graph in Figure 9 shows the return loss at ports 1, 2 and 3, which correspond to the input port, direct output port and the coupled port respectively. The graph shows that the return loss at all ports remains below -10 dB over the entire frequency spectrum and close to -15 dB around the frequency of interest. Overall, a low level of return loss is shown, thus demonstrating that the design specifications are met.

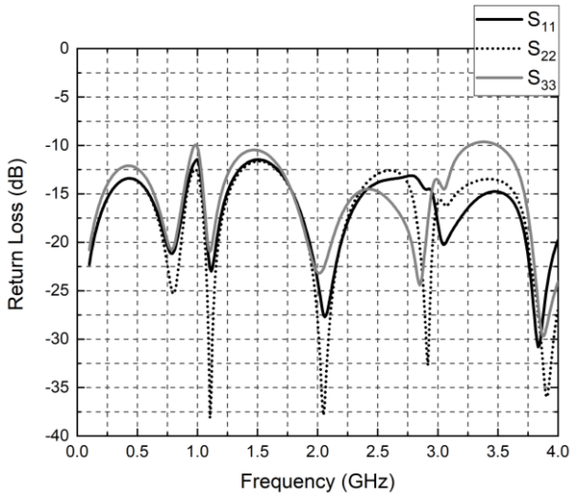

Figure 9 Return loss (dB), parameters S_{11}, S_{22}, S_{33} in a frequency range of 1 to 4 GHz

The graph in Figure 10 shows the insertion losses corresponding to parameter S_{12}, the coupling level in the parameter S_{13} and the isolation level on port 4 in parameter S_{14}. The graph shows that this parameter is above -5 dB over the entire frequency range sampled and between -1 and -2 dB around the frequency of interest, demonstrating that the coupler has low transmission losses from the input port to the direct port.

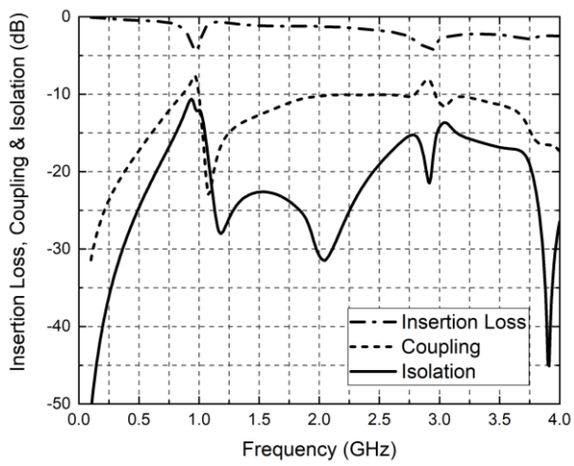

Figure 10 Insertion loss, coupling and isolation factor (dB), in a frequency range from 1 to 4 GHz

On the other hand, the blue curve shows how the coupling factor (coupling) remains at -10 dB for frequency values between 2 and 2.75 GHz. In turn, the isolation factor (isolation) is maintained at values below -15 dB in almost the entire frequency spectrum, with a minimum of -37 dB at 2 GHz; in general, good levels of both coupling and isolation are observed for the entire sampled range.

ISSN-On line: 2444-4987

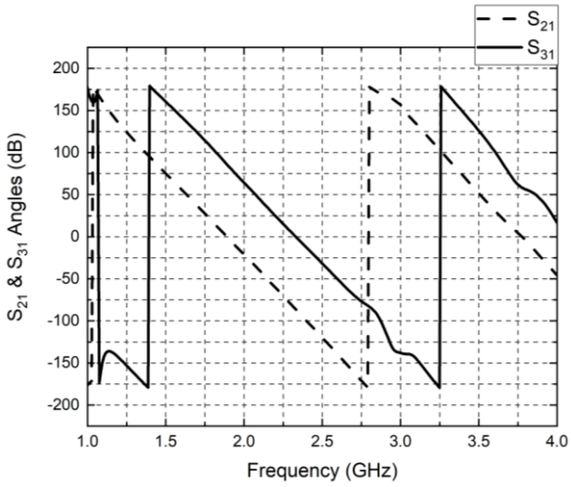

Figure 11 Angles of S_{12} y S_{13} expressed in degrees over a frequency range of 1 to 4 GHz

Finally, the angles of the parameters are S_{12} and S_{13} shown in degrees. In a directional coupler, there must be a phase shift of 90° between the output signal at port 2 and the coupled signal at port 3. From the graph in Figure 12, a phase shift close to 90° is observed between the two signals, a condition that is met for a range of 1.4 to 2.75 GHz.

Acknowledgements

The authors would like to thank the Tecnológico Nacional de México/Instituto Tecnológico de Ciudad Madero and the Consejo Nacional de Ciencia y Tecnología CONACyT for funding the development of this project.

Conclusions

From the analysis of the results obtained by simulation, a coupling factor of -10 dB is observed in the frequency range from 1.75 to 2.75 GHz. Also, it is observed that in the same range a good level of isolation is achieved at the frequency of interest, which remains below -15 dB in almost the entire sampled spectrum and at a value of -18 dB at the centre frequency. The return loss remains below -10 dB throughout the range, i.e. there are low levels of return loss. Furthermore, it can be observed that the power transferred to the direct port decreases by -1.8 dB with respect to the incident power and that the angle between the two signals is 4° above 90°, i.e. 4.4% of the ideal value.

This shows that the coupler complies with the specifications by presenting low insertion and return loss, a good level of coupling at the centre frequency (2.5 GHz) and a good level of isolation of less than -15 dB.

References

Avionics Department (2013). Power Dividers and Directional Couplers, *Electronic Warfare and Radar Systems Engineering Handbook*, Technical Communication Office, VI, 4, 276–281.

Chen, S. & Xue, Q. (2013). Compact triple-transistor Doherty amplifier designs: differential/power combining, *IEEE transactions on microwave theory and techniques*, 61(5), 1957–1963. https://doi.org/10.1109/TMTT.2013.2253794

Chen, X. P., Wu, K., Han, L. & He, F. (2010). Low-cost high gain planar antenna array for 60-GHz band applications, *IEEE Transactions on Antennas and Propagation*, 58(6), 2126–2129. https://doi.org/10.1109/TAP.2010.2046861

Du, C., Yang, Z., Jin, G., & Zhong, S. (2022). Design of a co-planar waveguide-fed flexible ultra-wideband-multiple-input multiple-output antenna with dual band-notched characteristics for wireless body area network. *International Journal of RF and Microwave Computer-Aided*

Edwards, T. C. (2016). Parallel-coupled Microstrip Lines, *Foundations for microstrip circuit design*, 4th ed. John Wiley & Sons, 10, 10.1-10.5, 268–304. https://doi.org/10.1002/9781118936160.ch10

He, Q., OuYang, P., Gao, H., Li, Y., Wang, Y., Chen, Y., ... & Wei, L. F. (2022). Low-loss superconducting aluminum microwave coplanar waveguide resonators on sapphires for the qubit readouts. *Superconductor Science and Technology*, 35, 6. http://dx.doi.org/10.1088/1361-6668/ac6a1d

Kim, D., Choi, H. Y., Allen, M. G., Kenney, J. S. & Kiesling, D. (2002). A wide bandwidth monolithic BST reflection-type phase shifter using a coplanar waveguide Lange coupler, *2002 IEEE MTT-S International Microwave Symposium Digest (Cat. No. 02CH37278)*, 3, 531–533.

https://doi.org/10.1109/MWSYM.2002.1012133

Liang, K. H., Chang, H. Y. & Chan, Y. J. (2007). A 0.5-7.5 GHz Ultra Low Voltage Low-Power Mixer Using Bulk-Injection Method by 0.18-um CMOS Technology, *IEEE Microwave and Wireless Components Letters*, 17(7), 531–533. https://doi.org/10.1109/LMWC.2007.899319

Liu, J. Y. C., Chen, J. S., Hsia, C., Yin, P. Y. & Lu, C. W. (2014). A wideband inductorless single-to-differential LNA in 0.18um CMOS technology for digital TV receivers, *IEEE microwave and wireless components letters*, 24(7), 472–474. https://doi.org/10.1109/LMWC.2014.2316495

Mousavi, S. M., Mirtaheri, S. A., Khosravani-Moghaddam, M. A., Habibi, B. & Meiguni, J. S. (2015). Design, fabrication and test of a broadband high, directivity directional coupler. *IEEE 23rd Iranian Conference on Electrical Engineering*, 168–170. http://dx.doi.org/10.1109/IranianCEE.2015.7146203

Roshani, S., Azizian, J., Roshani, S., Jamshidi, M. B., & Parandin, F. (2022). Design of a miniaturized branch line microstrip coupler with a simple structure using artificial neural network. *Frequenz*, 76(5-6). http://dx.doi.org/10.1515/freq-2021-0172

Shi, J. & Xue, Q. (2010). Balanced band pass filters using center-loaded half-wavelength resonators, *IEEE transactions on microwave theory and techniques*, 58(4), 970–977. https://doi.org/10.1109/TMTT.2010.2042839

Shi, J., Chen, J. X. & Xue, Q. (2008). A novel differential bandpass filter based on double-sided parallel-strip line dual-mode resonator, *Microwave and Optical Technology Letters*, 50(7), 1733–1735. https://doi.org/10.1002/mop.23493

Simons, R. N. (2001). Directional Couplers, Hybrids, and Magic T's *Coplanar Waveguide Circuits, Components, and Systems*, John Wiley & Sons,Inc. 165, 11, 11.2, 346–352. https://doi.org/10.1002/0471224758.ch11

Simons, R. N. (2001). Microshield Lines and Coupled Coplanar Waveguide, *Coplanar Waveguide Circuits, Components, and Systems*, Vol. 165. John Wiley & Sons, Inc 7, 7.4, 190–193. https://doi.org/10.1002/0471224758.ch7

Tessmann, A., Kuri, M., Riessle, M., Massler, H., Zink, M., Reinert, W. & Leuther, A. (2006). A compact W-band dual-channel receiver module *IEEE MTT-S International Microwave Symposium Digest*, 85–88. IEEE. https://doi.org/10.1109/MWSYM.2006.249934

Wadell, B. C. (1991). Coupled Lines. *Transmission line design handbook*, Artech House Microwave Library, IV, 4.4.3, 196–198.

Wane, S., Leyssenne, L., Tesson, O., Doussin, O., Bajon, D., Lesénéchal, D. & Erdem, A. (2015). Design of Lange Couplers with local ground references using SiGe BiCMOS technology for mm-Wave applications, 2015 *IEEE Radio Frequency Integrated Circuits Symposium (RFIC)*, 17(7), 351–354. https://doi.org/10.1109/RFIC.2015.7337777

Watson, P. M. & Gupta, K. C. (1997). Design and optimization of CPW circuits using EM-ANN models for CPW components, IEEE *Transactions on Microwave Theory and Techniques*, 45(12), 2515–2523. https://doi.org/10.1109/22.643868

Xiao, J. K., Zhu, M., Ma, J. G. & Hong, J. S. (2016). Conductor-backed CPW bandpass filters with electromagnetic couplings, *IEEE Microwave and Wireless Components Letters*, 26(6), 401–403. https://doi.org/10.1109/LMWC.2016.2562641

Yu, F., & Yang, X. X. (2022). Progress of Rectenna Arrays for Microwave Power Transmission Systems. *Advances in Astronautics Science and Technology*, 1-10. http://dx.doi.org/10.1007/s42423-022-00100-0

Zhao, Y., Dong, J., Yin, F., Fang, X., & Xiao, K. (2022). Broadband Coplanar Waveguide to Air-Filled Rectangular Waveguide Transition. *Electronics*, 11(7), 1057. http://dx.doi.org/10.3390/electronics11071057

ISSN-On line: 2444-4987